energies

MDPI

Review

Modelling Syngas Combustion from Biomass Gasification and Engine Applications: A Comprehensive Review

José Ramón Copa Rey, Andrei Longo, Bruna Rijo, Cecilia Mateos-Pedrero, Paulo Brito and Catarina Nobre *

VALORIZA–Research Centre for Endogenous Resource Valorization, Portalegre Polytechnic University, Campus Politécnico 10, 7300−555 Portalegre, Portugal; jose.rey@ipportalegre.pt (J.R.C.R.); andrei.longo@ipportalegre.pt (A.L.); cecilia.pedrero@ipportalegre.pt (C.M.-P.); pbrito@ipportalegre.pt (P.B.)
* Correspondence: catarina.nobre@ipportalegre.pt

Abstract

Syngas, a renewable fuel primarily composed of hydrogen and carbon monoxide, is emerging as a viable alternative to conventional fossil fuels in internal combustion engines (ICEs). Obtained mainly through the gasification of biomass and organic waste, syngas offers significant environmental benefits but also presents challenges due to its lower heating value and variable composition. This review establishes recent advances in understanding syngas combustion, chemical kinetics, and practical applications in spark-ignition (SI) and compression-ignition (CI) engines. Variability in syngas composition, dependent on feedstock and gasification conditions, strongly influences ignition behavior, flame stability, and emissions, demanding detailed kinetic models and adaptive engine control strategies. In SI engines, syngas can replace up to 100% of conventional fuel, typically at 20–30% reduced power output. CI engines generally require a pilot fuel representing 10–20% of total energy to start combustion, favoring dual-fuel (DF) operation for efficiency and emissions control. This work underlines the need to integrate advanced modelling approaches with experimental insights to optimize performance and meet emission targets. By addressing challenges of fuel variability and engine adaptation, syngas reveals promising potential as a clean fuel for future sustainable power generation and transport applications.

Keywords: syngas; biomass gasification; combustion kinetics; internal combustion engines; dual-fuel operation; modelling; emissions

Academic Editor: Albert Ratner

Received: 22 August 2025
Revised: 18 September 2025
Accepted: 23 September 2025
Published: 25 September 2025

Citation: Rey, J.R.C.; Longo, A.; Rijo, B.; Mateos-Pedrero, C.; Brito, P.; Nobre, C. Modelling Syngas Combustion from Biomass Gasification and Engine Applications: A Comprehensive Review. *Energies* **2025**, *18*, 5112. https://doi.org/10.3390/en18195112

1. Introduction

Global energy demand continues to rise, with fossil fuels still supplying over 80% of primary energy [1]. In contrast, renewable energy capacity is expanding rapidly, driven by cost reductions, investments, and technological advances. In 2024, renewables added 585 GW, accounting for 92.5% of all new power capacity, setting their place in global energy expansion. Among them, biomass thermochemical conversion remains critical for industrial applications, providing nearly 89% of renewable heat consumption in 2022 and emphasizing its importance beyond electricity generation [2].

Biomass and organic waste are renewable energy sources with neutral CO_2 emissions that play a key role in replacing traditional fossil fuels in the energy transition process. The origin and chemical composition of biomass are highly relevant factors in the final composition of the products from its valorisation [3]. In many cases, biomass requires pretreatment to achieve the necessary characteristics for efficient conversion by thermochemical methods.

Whether due to high moisture and ash content, the need for particle size reduction, or the presence of undesirable mineral compounds, among other factors, the characteristics of the raw residue are fundamental in determining the efficiency and economic viability of its valorisation through the gasification process [4].

Raw biomass is typically characterized by high moisture contents, particularly in non-lignocellulosic residues from agriculture, livestock waste, residues from microalgae cultivation, and sewage sludge [5]. In the case of the latter, the high ash content and its composition can pose barriers to the gasification process due to the formation of fouling and slagging, as well as the emission of compounds that harm the environment and human health [6].

Lignocellulosic biomass wastes are characterized by high lignin content and are mainly derived from forest residues, agricultural leftovers, and energy crops. For H_2 production, this feedstock may result in a higher concentration in the syngas output and increased economic viability compared to other biomass waste streams [7]. This type of biomass has great potential for achieving high efficiency in the gasification process, particularly in samples with a moisture content of less than 20% and in the presence of catalysts. The degradation of lignin enhances H_2 production, resulting in increased char and gas production, rather than tar formation, which is promoted by the cellulose and hemicellulose content. It makes woody biomass waste from agricultural and forestry activities a potential feedstock for highly efficient syngas production through catalytic steam gasification [8].

Non-woody biomass waste also represents a potential source of renewable energy in rural areas, as it is abundant, readily available, and inexpensive and poses a significant challenge in the waste management context. It is primarily represented by agricultural byproducts and herbaceous waste resulting from agricultural activities. Although this biomass fraction is less efficient than lignocellulosic ones for valorisation in the gasification process, it requires less energy for pretreatment and may appear as a viable energy source for small-scale producers. Moreover, co-gasification of these wastes with coal or biochar may enhance the quality of syngas and improve process efficiency [9].

Other non-woody biomass waste streams have also shown potential for valorisation through gasification. Microalgae biomass is reported to yield a H_2-rich syngas through catalytic gasification with increased efficiency under higher temperatures [10]. Furthermore, the organic composition of microalgae plays a crucial role in determining the yield and composition of syngas, where lipids are positively correlated with H_2 production, whereas carbohydrates exhibit the opposite trend and are also linked to CO yield [11]. Sewage sludge has also been described as a potential feedstock for high-added-value products through gasification. Due to its challenging composition, usual methods for its valorisation face several constraints, mainly related to soil contamination and increased costs for disposal and treatment [12]. In this context, sewage sludge gasification is positioned as a promising technology to address the drawbacks of conventional disposal and the limitations of incineration. The high organic matter content makes it suitable for the production of added-value products, whereas the inorganic ash content may partially replace the chemical fertilizers in the agricultural processes [13].

Within biomass conversion pathways, thermal gasification plays a central role. This process partially oxidizes carbon-based feedstocks with limited oxidants such as air, oxygen, or steam, producing a combustible mixture of hydrogen, carbon monoxide, and methane, commonly known as syngas, rather than complete combustion products like CO_2 and H_2O [14]. After suitable cleaning and conditioning, syngas can be used in internal combustion engines (ICEs) for electricity generation [15]. Compared to other biomass-derived fuels, syngas offers clean combustion, multimodal fuelling flexibility, and relatively easy ICE integration. In spark-ignition (SI) engines, only minor modifications such as intake

manifold or throttle adjustments are needed, while in compression-ignition (CI) engines, its high auto-ignition temperature typically requires dual-fuel (DF) operation with diesel pilot injection [16]. Empirical and numerical studies have reported significant benefits from syngas–diesel DF strategies, including reduced NO_x and particulate emissions, albeit sometimes accompanied by increased CO, total hydrocarbons, or reduced brake power [17–20].

As global trends increasingly favour electrification, internal combustion engines (ICEs) still play a vital role in many transportation and industrial sectors. Passenger vehicles, shipping, aviation, agriculture, and construction heavily rely on ICE technology, as achieving full electrification poses significant technical and economic challenges.

The current scenario stresses the need to enhance ICE performance and emissions control. Syngas, a renewable and low-carbon fuel that offers flexibility, represents a viable solution for reducing greenhouse gas emissions while utilising existing ICE infrastructure and enabling hybrid or dual-fuel strategies [21,22].

Recent advances have expanded both fundamental and applied understanding of syngas utilization. Modelling frameworks increasingly integrate machine learning with computational fluid dynamics (CFD) to predict gasifier performance and syngas yields across diverse configurations. Catalyst development, such as stable Ni/Ca_3AlO systems, has demonstrated improved hydrogen-rich syngas production and durability under steam gasification conditions [23,24]. At the system level, downdraft gasifiers remain among the most efficient and mature technologies for small-scale electricity generation, producing syngas with tar and particle contents typically below 100 mg/Nm^3 and 50 mg/Nm^3, respectively [25]. Techno-economic analyses show that downdraft gasifier–ICE systems can achieve overall efficiencies of 13–14%, making them viable for decentralized electrification in rural and forested regions [26,27]. In parallel, recent works emphasize the integration of automation, AI-based process control, and sustainability metrics to optimize biomass-to-syngas pathways [28].

This work stands out from previous reviews by integrating a comprehensive comparison of biomass gasification fundamentals, syngas conditioning, combustion kinetics, and internal combustion engine (ICE) performance. This study offers a renewed and holistic perspective by comparing experimental findings with kinetic models and incorporating innovative tools, such as integrating computational fluid dynamics (CFD) with machine learning and hybrid fuelling strategies. This insight aims to guide realistic and scalable applications of syngas in engines.

2. Gasification-Based Syngas Production

2.1. Gasification Process

Gasification is a thermochemical conversion route that transforms carbon-rich feedstocks such as biomass, municipal solid waste (MSW), or coal into syngas primarily composed of hydrogen, carbon monoxide, and smaller fractions of methane, carbon dioxide, and inert gases. This process occurs under oxygen-limited conditions, enabling partial oxidation rather than complete combustion and thus retaining much of the chemical energy within the fuel gas. Understanding these core principles helps contextualize the role of gasification as a vital technology for sustainable energy production. Recent studies highlight gasification's contribution to decarbonizing power and transport sectors, especially when combined with carbon capture or renewable hydrogen initiatives [29,30]. The typical composition and lower heating value (LHV) of syngas vary with the gasification agent, as summarized in Table 1, where steam and oxygen use generally yield higher LHV than air-based systems [31–35].

Table 1. Typical syngas composition and LHV depending on the gasification agent.

Gasifying Agent	H_2 (vol%)	CO (vol%)	CO_2 (vol%)	CH_4 (vol%)	N_2 (vol%)	LHV ($MJ \cdot Nm^{-3}$)	Ref.
Air	8–18	15–25	5–15	0–3	45–55	4–7	[32,34]
Oxygen	20–30	45–55	5–15	0–5	0–3	10–12	[31,32]
Steam	40–55	15–25	5–12	2–6	0–3	12–14	[32,33]
Oxygen–steam	30–45	35–50	5–12	1–5	0–3	10–14	[31,35]

The conversion process occurs through overlapping stages, namely, drying, pyrolysis, oxidation, and reduction, rather than sharply separated steps. Drying, typically between 100 °C and 200 °C, removes inherent moisture from the feedstock, improving thermal efficiency. Pyrolysis then decomposes organic matter into volatiles, condensable tars, and char at 300–700 °C. In the oxidation zone, exothermic reactions generate heat to sustain endothermic reduction reactions, where char reacts with steam and CO_2 to form CO and H_2 via the water–gas and Boudouard reactions. Methane reforming and water–gas shift (WGS) reactions further adjust the final syngas composition [15,33,36]. The main chemical pathways are detailed in Table 2.

Table 2. Main reactions of the gasification process.

Reaction Name	Mechanism	ΔH_R^{298K}/kJ.mol^{-1}
Reactions of combustion	$C + 0.5O_2 \rightarrow CO$ $CO + 0.5O_2 \rightarrow CO_2$ $C + O_2 \rightarrow CO_2$ $H_2 + ½O_2 \rightarrow H_2O$	−111 −283 −393 −242
Boudouard reaction	$C + CO_2 \rightarrow 2CO$	+172
Water gas reaction	$C + H_2O \leftrightarrow CO + H_2$	+131
Water gas shift reaction	$CO + H_2O \leftrightarrow CO_2 + H_2$	−41
Methanation reactions	$C + 3H_2 \leftrightarrow CH_4$ $CO + 3H_2 \leftrightarrow CH_4 + H_2O$ $CO_2 + 4H_2 \leftrightarrow CH_4 + H_2O$	−75 −206 −165
Reforming of methane with steam	$CH_4 + H_2O = CO + 3H_2$	+206
Partial oxidation of methane	$CH_4 + 0.5O_2 = CO + 2H_2$	−36
Reforming of methane with CO_2	$CH_4 + CO_2 = 2CO + 2H_2$	+247

Figure 1 illustrates the sequence and interplay between these thermal and chemical stages within the reactor.

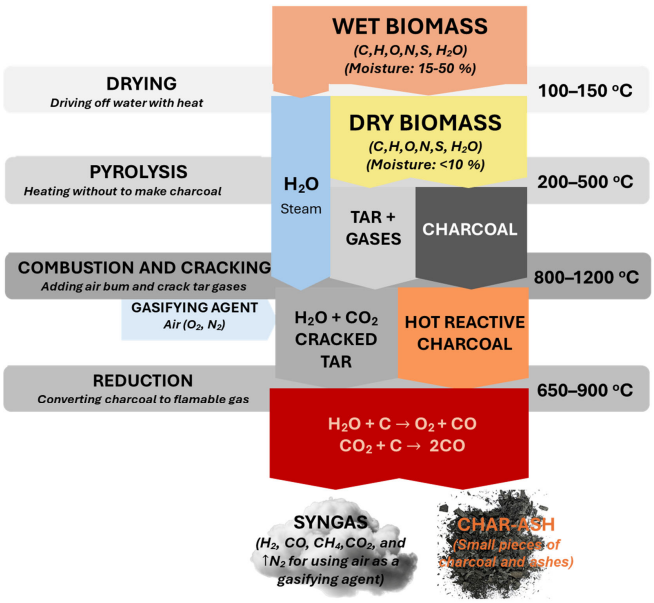

Figure 1. Main reactions and steps of the gasification process (adapted from [37]).

Gasifier configuration has a strong influence on efficiency, syngas quality, and applicability. Fixed-bed systems, particularly downdraft designs, are favored for small-scale power generation because they produce relatively low tar levels (<100 mg/Nm^3) and are mechanically simple to operate, though they require uniform, low-moisture feedstock [38,39]. Fluidized-bed reactors, in bubbling or circulating configurations, offer higher throughput, better temperature control, and fuel flexibility, but they produce more tars and particulates, requiring additional cleaning stages. Entrained-flow gasifiers achieve nearly complete carbon conversion and tar-free gas but demand finely milled feedstock and high operating pressures. Novel approaches such as plasma gasification and chemical looping gasification (CLG) have emerged, with the latter achieving carbon conversion efficiencies above 90% in recent pilot trials [40–42].

Operational parameters are critical for performance optimization. For fixed-bed biomass gasifiers, optimal operating temperatures are in the range of 700–900 °C, with equivalence ratios between 0.2 and 0.4 to balance conversion efficiency, tar minimization, and syngas LHV [43–45]. Excess moisture (>30%) lowers reactor temperature, increases tar formation, and reduces cold-gas efficiency (CGE). Likewise, high ash content feedstocks (e.g., rice husks) can limit usable energy yield and promote slagging, affecting long-term operation [46]. The influence of feedstock properties is illustrated in Table 3, which outlines proximate and ultimate composition for representative biomass types.

Table 3. Ultimate and proximate composition of different biomass types.

Biomass	Ultimate Analysis (wt.%)					Proximate Analysis (wt.%)				LHV (MJ/kg)	Ref.
	C	H	O	N	S	FC	VM	Ash	W		
Wood chips	49.6	6.0	43.8	0.5	0.1	10.7	49.1	1.4	38.7	9.9	[47]
Rubber wood	50.0	6.5	42.0	0.2	–	19.2	80.1	0.7	–	–	[48]
Wood	50.4	5.9	43.3	<0.1	<0.01	–	–	0.3	–	19.0	[27]
Eucalyptus	49.0	6.3	44.4	0.2	0.1	15.2	72.7	0.8	11.3	18.4	[49]
MSW Portugal	49.7	7.2	41.6	0.8	0.7	5.1	74.1	14.3	6.5	19.6	[50]
MSW Brazil	48.0	6.3	43.6	1.4	0.7	5.5	75.2	8.6	10.7	14.4	[51]
Switchgrass	49.6	5.7	40.4	0.3	0.05	17.5	78.6	3.9	7.7	16.5	[52]
Hazelnut shells	45.9	5.7	48.2	0.1	0.01	18.2	68.2	1.1	12.4	17.4	[53]
Sugarcane straw	44.8	5.9	48.9	0.1	0.3	13.3	77.3	9.6	0.9	15.7	[54]
Rice husk	40.8	5.3	53.4	0.4	0.2	16.4	61.8	20.9	0.9	14.9	
RDF pellets	71.5	10.7	17.0	0.7	0.1	4.4	74.9	16.5	4.3	25.7	[47]
Microalgae	50.9	7.0	31.0	10.2	0.8	12.6	80.7	6.7	–	20.8	[55]
Sewage sludge	52.3	7.9	32.6	6.4	0.8	10.6	72.3	17.1	–	18.6	[55]

Recent advances focus on modeling and intelligent control to improve system predictability and adaptability. CFD simulations resolve flow and reaction patterns in complex geometries, while data-driven and machine learning approaches can optimize operational parameters in real time according to feedstock and load variations [56,57]. These integrated strategies enable more accurate prediction of syngas composition and yield, supporting adaptive control in downstream applications such as ICEs and gas turbines. Table 4 gathers representative studies and approaches aligned with these advances, presenting hybrid modeling frameworks, optimization strategies, and supporting more accurate prediction and adaptive operation in gasification systems.

Table 4. Recent modeling and intelligent control approaches for gasification.

Focus	Modeling or Control Approach	Insights	Ref.
Hybrid modeling	Aspen Plus + Machine learning (ML)	Enhanced prediction accuracy	[58]
ML optimization	Gradient boosting	Impact of temperature and feedstock	[59]
CFD modeling	ANSYS Fluent	Reactor design strategies	[60]
ML combined with Explainable Artificial Intelligence (XAI)	XGBoost, SHAP/LIME	Improving syngas yield and feedstock quality	[61]
Hybrid ML and mechanistic modeling	GBR + Aspen Plus	Optimization of H_2−enriched syngas production	[62]

2.2. Gasifier Type

The vessel where gasification occurs is referred to as the gasifier. Several configurations exist, but most biomass gasification research focuses on four main categories: fixed-bed (updraft and downdraft), fluidized-bed (bubbling and circulating), entrained-flow, and plasma gasifiers (Figure 2). Globally, downdraft fixed-bed units account for roughly 75% of installed systems, followed by bubbling fluidized beds at about 20%, with the remaining 5% attributed to other designs [38,63].

Fixed-bed reactors are among the simplest gasification technologies, suitable for operation with different gasifying agents. They typically exhibit residence times between 900 and 1800 s, operate under pressures from 1 to 100 bar, and at temperatures ranging from 500 °C to 1200 °C. In updraft configurations (Figure 2a, left), biomass is introduced at the top with the gasifying agent entering from the bottom or side, and syngas exits from the top. This design yields high thermal efficiency but also higher tar levels. Downdraft gasifiers (Figure 2a, right) introduce both the feedstock and gasifying agent from the top or side, with syngas exiting at the bottom. Downdraft units achieve low tar concentrations (1–2 g/Nm^3) and high carbon conversion, making them optimal for small-scale combined heat and power (CHP) applications. However, they require uniform feedstock (<25% moisture, <15% ash), restricting large-scale deployment [38,63].

Entrained-flow gasifiers (Figure 2b) are widely used in industrial coal gasification but can be adapted for biomass. These require fine particles (0.1–1 mm), high temperatures (1300–1500 °C), and high pressures (25–30 bar) with short residence times. Advantages include nearly complete fuel conversion and tar-free syngas, while disadvantages include costly feedstock preparation [43].

Fluidized-bed reactors use an inert material (often silica sand), fluidized by a gasifying agent fed through a bottom distribution grid (Figure 2c). Biomass is added just above the grid, ensuring high heat transfer and uniform temperature. Bubbling beds operate at 1–3 m/s and 800–1000 °C, separating solids from syngas via cyclones. Circulating beds use higher velocities (3–10 m/s), allowing continuous recirculation and improved fuel conversion. These types are promising for large-scale biomass energy due to their flexibility and efficiency, though syngas quality is often lower (higher tar and particulates) [44,64].

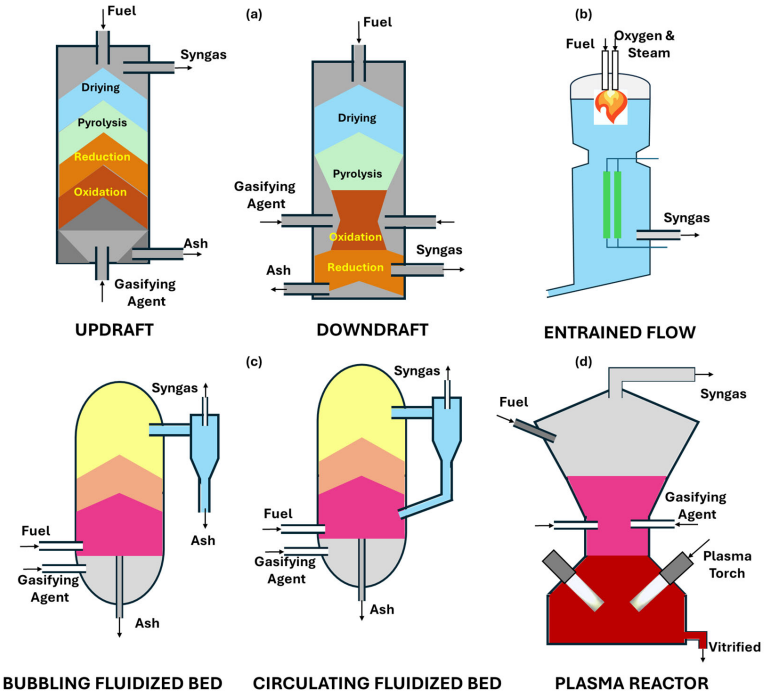

Figure 2. Schematic illustration of different types of gasifiers: (**a**) Fixed bed (left: updraft and right: downdraft); (**b**) Entrained flow; (**c**) Fluidized bed (left: bubbling fluidized bed and right: circulating fluidized), and (**d**) Plasma gasification.

Plasma gasification (Figure 2d) uses a high-temperature ionized gas (plasma) generated by electric arcs, reaching up to 10,000 °C. This process breaks down organic material into syngas and vitrifies inorganics into inert slag. Plasma systems can process diverse, minimally pre-treated feedstocks, yielding very clean gas, but high energy consumption increases operational costs [65].

The quality and composition of syngas produced through gasification critically determine its combustion characteristics and behavior in energy systems. Variations in the concentrations of hydrogen, carbon monoxide, methane, and diluents substantially influence ignition properties, flame stability, and pollutant formation. Understanding these combustion kinetics is essential for accurately predicting syngas performance in practical applications, motivating the detailed analysis presented in the following section.

2.3. Critical Insights on Syngas Production

While gasification provides a flexible pathway for producing syngas from diverse feedstocks, the literature shows substantial variations and inconsistencies. For instance, air-blown gasifiers yield nitrogen-diluted syngas with relatively low heating values (≈4–6 MJ/Nm^3), whereas oxygen- or steam-blown systems generate hydrogen-rich syngas with higher calorific values (≈10–15 MJ/Nm^3) [33]. This variability directly affects combustion behaviour and complicates comparisons between engine studies, many of which use idealised or synthetic mixtures that are not representative of practical gasification outputs.

Contradictions also emerge in reported hydrogen yields: some studies highlight significant increases in H_2 fraction with steam/oxygen gasification [66], while others report only marginal gains, which may be attributed to differences in feedstock composition, reactor type, and operating parameters. For example, MSW gasification introduces additional uncertainty due to its highly heterogeneous nature, often leading to wide-ranging CO_2 and CH_4 concentrations.

A further methodological limitation is that many engine studies rely on fixed syngas compositions, whereas in practice, syngas composition fluctuates dynamically with

operating conditions. This gap underscores the need for closer integration between gasification process modelling and engine combustion simulations to ensure realistic boundary conditions.

3. The Oxidation and Combustion Kinetics of Syngas

The oxidation and combustion kinetics of syngas are critical factors in determining its suitability as a fuel for ICEs and other advanced energy systems. Syngas composition varies widely depending on feedstock type, gasification technology, and operating conditions, with the primary combustible components being H_2, CO, and CH_4 [67,68]. This variability significantly influences ignition delay, flame stability, pollutant formation, and thermal efficiency. Therefore, reliable chemical kinetic models are essential for predicting performance and designing combustion systems across diverse operating conditions.

Combustion processes in syngas are also strongly influenced by dilution effects, arising from non-combustible species such as N_2 and CO_2 introduced during gasification [69]. These diluents reduce flame temperatures, alter radical pool dynamics, and impact pollutant emissions, particularly NOx. Understanding the interplay between fuel composition, reaction kinetics, and dilution effects is key to optimizing syngas utilization in ICEs, gas turbines, and industrial burners.

3.1. Experimental Characterization of Syngas Combustion

Variability in syngas composition presents challenges for combustion systems, including unstable operation, hot spots, and accelerated wear of hardware [70,71]. Fundamental combustion parameters such as ignition delay, laminar flame speed (LFS), and turbulent flame speed (TFS) are vital for mechanism validation and for designing combustion chambers that maintain stability and efficiency [72].

The laminar burning velocity provides insight into the intrinsic chemical reactivity of a mixture and is directly affected by hydrogen content. Bhaduri et al. [73] found that moisture in syngas prolongs ignition delay in homogeneous charge compression ignition (HCCI) engines, whereas tars exert a negligible influence. Experimental studies confirm that laminar flame speed increases with higher hydrogen content in syngas, particularly when H_2 exceeds ~20 vol.% [33], (see Figure 3). This effect improves ignition stability and lean-burn operability within the practical range for biomass-derived syngas (10–40 vol.% H_2). Hydrogen fractions above 50–60% are seldom achieved in real gasification processes and are therefore not directly relevant to typical syngas-fueled engines [74].

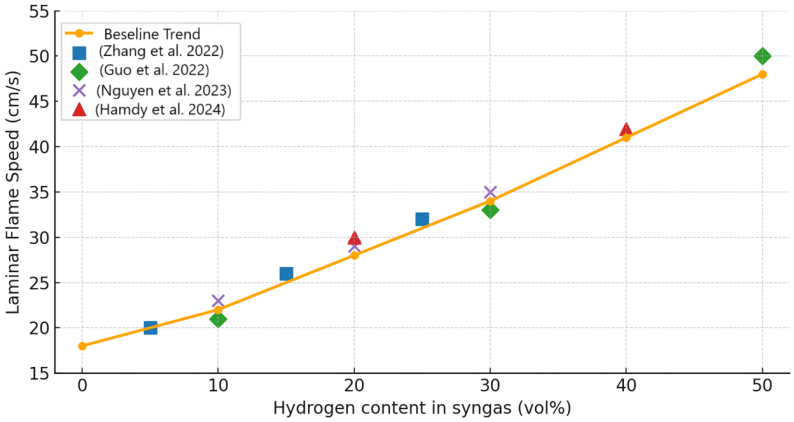

Figure 3. Laminar Flame Speed as a Function of Hydrogen Content in Typical Biomass-Derived Syngas (≤50 vol%). Orange line: baseline trend. Scatter markers: literature data [75–78]. Values plotted are approximate and based on reported trends.

TFS, which governs flame propagation under engine-relevant conditions, reflects the interaction between laminar flame fronts and turbulent eddies. Yin et al. [67] measured TFS for a 35:65 H_2:CO mixture at ϕ = 0.5–0.7 over pressures from 1 to 10 bar, observing that TFS $\sim p^{0.15}$ for ϕ = 0.7 and TFS $\sim p^{0.11}$ for ϕ = 0.5. At higher pressures (up to 20 bar), Wang et al. [79] linked further increases in TFS to combined diffusive–thermal and hydrodynamic instabilities, consistent with high-hydrogen syngas behavior reported by Zhao et al. [80].

Dilution gases significantly alter syngas combustion. Shang [69] found that hydrogen-rich flames produce higher NO emissions than hydrogen-lean flames under similar conditions due to elevated flame temperatures. Uka et al. [81] demonstrated that CO_2 dilution suppresses LFS more effectively than N_2 due to its higher heat capacity and radical scavenging capability. Hu et al. [82] reported that the Davis mechanism matches experimental results well for medium-and high$-H_2$ fuels at preheat temperatures up to 500 K, but overestimates LFS at higher preheat levels.

3.2. Modelling and Kinetic Mechanisms of Syngas Combustion

To date, researchers have developed numerous combustion kinetic models to describe syngas oxidation and its application in engine simulations. These models initially consider the combustion mechanisms of the main fuel components of syngas, namely H_2, CO, and CH_4. Burke, Dryer, and Ju [83] conducted modelling of mixtures consisting of $H_2/CH_4/O_2$/diluents under a wide range of conditions, including an equivalence ratio of 0.30 to 1.0, flame temperatures of 1400 to 1800 K, and pressures of 1 to 25 bar. They discovered that in lean flames, the impact of pressure on the kinetics was primarily driven by the competition between main branching reactions and both H + O_2 + M = HO_2 + M (M represents any inert molecule in the atmosphere, typically N_2, which serves as a medium for dissipating excess energy) and HO_2 + O/OH/HO_2. However, in rich mixtures, the effect of pressure on the kinetics was influenced by the competition of both H + O_2 + M = HO_2 + M and HO_2 + H with the main branching reactions. The pressure dependence of the flames, in the presence of CH_4, was predominantly determined by the reactions of CH_3 with H and HO_2.

Kéromnès et al. [84] proposed a detailed chemical kinetic model for the oxidation of a hydrogen and syngas mixture, investigating pressures ranging from 1 to 70 bar, temperatures from 914 to 2220 K, and inequivalence ratios of 0.1 to 4.0. The authors observed that the mixture's reactivity was governed by hydrogen chemistry when the CO concentrations in the fuel mixture were below 50%. At higher CO concentrations, an inhibitory effect of CO was observed. Additionally, they developed a comprehensive chemical kinetic mechanism for hydrogen and H_2/CO mixtures, adjusting the rate constants to reflect newly obtained experimental information at high pressures. In their chemical kinetic model, the reaction $H_2 + H\dot{O}_2 \leftrightarrow \dot{H} + H_2O_2$ followed by the reaction $H_2O_2(+M) \leftrightarrow \dot{O}H + \dot{O}H(+M)$, was found to play a crucial role in hydrogen ignition under high-pressure and intermediate-temperature conditions. Conversely, at low pressure (1 atm) and low temperature (below 1000 K), the reactivity was mainly controlled by the competition between the chain-branching reaction $\dot{H}_2 + O_2 \leftrightarrow \ddot{O} + \dot{O}H$ and the pressure-dependent chain-propagating reaction $\dot{H} + O_2(+M) \leftrightarrow H\dot{O}_2(+M)$.

Li et al. [85] identified that the existing H_2/CO kinetic models failed to accurately predict the LFS of $H_2/O_2/CO_2$ mixtures at high pressures. To investigate the discrepancy, an uncertainty analysis was performed using the data collaboration method, revealing inconsistencies in the existing data. To address these issues, new experiments were conducted under similar conditions, and the newly obtained values were consistent with other data in the dataset. Therefore, it is recommended to enhance the performance and design of the model for improved predictions.

Olm et al. [86] analysed experimental results of syngas combustion in fast compression machines over the past decade. Among the findings, a delay in ignition times for temperatures below 1000 K was observed. The accuracy in reproducing ignition delay times did not significantly change with pressure, and the measured and simulated LFS were better at low initial temperatures for mixtures rich in CO and highly diluted. Costa et al. [87] presented a numerical model for simulating CI engine operating in DF mode with syngas and biodiesel. The model results indicated that high percentages of syngas decrease combustion efficiency in the engine while increasing thermal efficiency. Moreover, the use of syngas reduced the formation of NO but increased the presence of CO and soot compared to the use of pure biodiesel.

Wiemann et al. [88] conducted experimental analysis and simulated the combustion of syngas in a single-cylinder engine, investigating its effects on both SI and HCCI engines. The experimental results and simulations exhibited good agreement overall. The data revealed comparable work and heat transfer from the engine for lean and moderately rich combustion. Hence, both combustion methods were deemed suitable for adjusting power generation in a stationary engine. Rinaldini et al. [18] performed a numerical analysis of combustion in an indirect CI injection engine fuelled by diesel and syngas. The CFD model incorporated a scheme of chemical kinetics adapted to the combustion of DF. The model results indicated that modifying the beginning of the injection angle is necessary to preserve the mechanical integrity of the engine and maximize its braking efficiency. The numerical analysis provides guidelines for establishing the injection strategy based on the distribution of syngas.

Recent studies have advanced our understanding of engine performance by utilising full engine-cycle simulations with realistic syngas compositions derived from biomass gasification, which typically contain up to 50% hydrogen. For example, Costa et al. [89] applied 3D computational fluid dynamics (CFD) to a biomass-fuelled micro-combined heat and power (CHP) spark-ignition (SI) engine. Their findings showed that using inert gases for dilution, such as CO_2 and N_2, decreases the lower heating value (LHV) and in-cylinder temperature. However, a moderate concentration of hydrogen (20–30 vol.%) helps maintain efficiency.

In another study, Gordillo and González [90] utilised the KIVA−4 model, coupled with detailed chemical kinetics, to optimise the performance of syngas in SI engines. They demonstrated that increasing the amount of hydrogen reduces the ignition delay, while CO_2 dilution lowers the flame temperature and nitrogen oxides (NOx) emissions.

Gao et al. [33] systematically synthesised data regarding typical syngas compositions from gasifiers, underscoring their significance as realistic inputs for CFD and kinetic models. In the context of compression ignition (CI) engines, Perrone and Costa [91] modelled the direct injection of biomass-derived syngas in a micro-CHP CI engine, reporting high efficiency and reduced NOx emissions during direct injection operation.

Table 5 summarizes key studies, detailing simulation methods, engine types, fuel compositions, objectives, and principal findings on syngas combustion.

Insights gained from experimental and modelling studies of syngas combustion kinetics directly inform the development and optimization of ICE fueled by syngas. Knowledge of ignition delays, flame speeds, and emissions behavior shapes engine design choices and combustion control strategies. The following section explores how these kinetic principles translate into practical applications within SI and CI engines, highlighting challenges and current advancements.

Table 5. Summary of the key research papers published about syngas combustion modelling in different types of ICE (e.g., SI, CI, and HCCI variations).

Engine Type	Simulation Method	Engine/Experimental Info	Fuel Composition (% vol.)	Objective(s)	Finding(s)	Ref.
SI	KIVA4–CHEMKIN	4–stroke, 4–cyl SI engine, CR = 12.9:1, rpm = 1500, ϕ = 0.8, IT variable	SG: H2 17; CO 15; CH4 4; CO2 15; O 0.14; N2 53Biogas: CH4 65; CO2 35	Effects of IT, H2, and CH4 contents on SI engine fueled with SG and biogas	Under WOT and MBT: ITE: SG 39% > Biogas 37.5%; NOx: SG 3.3 g/kWh < Biogas 7.2 g/kWh. At advanced ITs: ↑ H2 (11–20%) less sensitive to NOx than ↑CH4 (55–88%)	[92]
SI	3D CFD (engine cycle, detailed kinetics)	Biomass-fueled micro-CHP SI engine	H2 20–30; CO 25–40; CO2/N2 balance	Assess syngas composition effects on engine thermal balance	Inert dilution (CO2/N2) ↓ LHV & cylinder temps; moderate H2 supports efficient operation	[66]
SI	3D CFD (KIVA–4 + GRI−Mech 3.0)	SI engine, full-cycle CFD	H2 15–35; CO 20–40; CO2 10–20; CH4 2–5	Optimize SI engine performance with biomass syngas	↑ H2 → faster ignition; CO2 dilution → ↓ flame temp & NOx	[90]
SI	Data synthesis + CFD benchmarking	Typical gasifier syngas ranges; validation for CFD	H2 20–30; CO 25–45; CO2 5–15; CH4 0–5	Provide realistic syngas input data for kinetic/CFD models	Steam/oxy-steam gasification ↑ H2 fraction & LHV; air-blown yields low H2, high N2	[33]
SI	Multidimensional CFD + kinetic analysis	SI engine conditions, syngas blends with variable CO/H2	H2 15–30; CO 20–40; CH4 0–5; balance inerts	Quantify impact of CO/H2 ratio and diluents	↑ H2 → shorter ignition delay & ↑ reactivity; CO ensures flame stability	[93]
SI	CHEMKIN	4–stroke, 2–cyl SI research engine, CR = 11:1, 1500 rpm	SG: H2 12.8–37.2; CO 11.5–16.4; CH4 2.3–3.6; CO2 10.8–24.7; N2 18.1–62.6	Model impact of H2 fraction on energy balance & efficiency	↑H2 12.8→19.4% → ↑ brake thermal efficiency; ↑ H2 up to 37.2% → ↓ brake thermal efficiency	[94]
CI (retrofitted to SI)	2−D thermodynamic code + PHOENICS	4–stroke, 6–cyl CI engine, CR = 16.3 (CI mode), 1100 rpm	SG: H2 6; CO 25; CH4 5; CO2 11; N2 53	Simulate SG combustion in CI engines used in SI mode	Predicts primary parameters of SG combustion in adapted CI engines	[95]
CI (retrofitted to SI)	Zero-dimensional model	4–stroke, 6–cyl CI engine, CR = 16.5 (CI), 10.5 (SI), rpm = 1500	SG: H2 19; CO 19; CH4 2; CO2 12; H2O 2; N2 46	Assess SG impact on engine performance with turbocharger	Imbalance in turbocharger → ↓ engine power; optimization can mitigate losses	[96]
CI	1–D multicylinder engine model (GT-SUITE)	4–stroke, 1–cyl CI engine, CR = 15:1, rpm = 1800	SG: H2 70; CO 15; CO2 15	Evaluate SI engine feasibility with H_2–rich SG	15% fuel consumption reduction vs. NG bus; ↓ thermal efficiency under high load	[97]
CI	3D CFD (engine simulation, DI syngas)	Micro-CHP CI engine	H2 22–30; CO 28–38; CO2 8–12; CH4 2–4; N2 balance	Evaluate direct injection of biomass syngas in CI engines	High efficiency & reduced NOx under DI syngas	[89]
DF (Diesel/Syngas)	3D CONVERGE CFD	4–stroke, 1–cyl Ricardo Hydra CI engine, CR = 15.5:1, rpm = 1200	Main fuel: Diesel; SG: H2 3; CO 11; CO2 3.4; CH4 1.4; C2H4 2.9; N2 78.2	Study RCCI with diesel & reformed diesel	↑ ITE, ↓ NOx, ↓ THC, ↑ controllability, ↑ CO & CO2	[98]
DF (Diesel/Producer Gas)	Heat Release Rate model (CONVERGE)	4−stroke, 1–cyl Yanmar CI engine, CR = 20.9:1	Main fuel: Diesel; PG: H2 15; CO 20; CH4 4; CO2 12; O2 1; N2 48	Effect of PG substitution of diesel on HRR & combustion	PG/diesel: delayed combustion start, ↓ max BTE, ↓ max pressure, ↓ NOx	[99]
HCCI	Zero-dimensional single-zone thermochemical model	HCCI engine	SG: H2 50; CO 50	Improve HCCI combustion with ozone or excited oxygen	Ignition accelerated before TDC → ↓ intake temperature; 1% singlet delta oxygen ↑ power 7–14%	[100]
HCCI	Multi-zone model + semi-detailed kinetics	4–stroke, 1–cyl Waukesha CFR engine, CR = 11.5–19:1, rpm = 800	Main fuel: PRFs; SG: 0–30% replacement, H2/CO = 1/1	Effect of syngas addition on HCCI performance	↓ H2 abstraction rate, ↑ fuel decomposition time, ↓ combustion start, ↓ peak pressure/temp, ↓ NOx, ↑ HC & CO	[101]

Denotations: ↑: increase; ↓: decrease; IMEP: Indicated Mean Effective Pressure; CR: Compression Ratio; ITE: Indicated Thermal Efficiency; BTE: Brake Thermal Efficiency; CoV IMEP: Coefficient of Variation of IMEP; PRF: Primary Reference Fuel; SOC: Start of Combustion; ϕ: The fuel/air equivalence ratio; WOT: Wide Open Throttle, and MBT: Maximum Brake Torque; HC: Hydrocarbons; THC: Total Hydrocarbons.

3.3. Critical Insights on Kinetic Modelling

Significant progress has been made in developing detailed kinetic mechanisms for syngas combustion; however, contradictions exist between model predictions and experimental data. For instance, Kéromnès et al. [84] demonstrated that hydrogen chemistry dominates reactivity when carbon monoxide (CO) content is below 50%. In contrast, Li et al. [85] found that existing H_2/CO mechanisms tend to underestimate laminar flame speeds in CO_2–diluted mixtures at elevated pressures. Similarly, Olm et al. [86] noted a consistent underprediction of ignition delay at low temperatures (below 1000 K), particularly for CO–rich mixtures. These discrepancies indicate that current mechanisms are unreliable across the full range of engine-relevant conditions.

Another challenge is that many validation datasets are limited to simplified mixtures, such as H_2/CO/CH_4 in O_2/Air or N_2 diluents, whereas practical syngas often contains significant amounts of CO_2 and trace hydrocarbons [102]. Consequently, extrapolating these models to real biomass-derived syngas may introduce errors. Furthermore, most kinetic models have been developed under controlled laboratory conditions (constant pressure and homogeneous mixtures) that do not accurately reflect internal combustion engines' turbulence, stratification, and transient pressures [103].

Despite their complexity, current kinetic mechanisms need refinement and validation under high-pressure, low-temperature, and diluted conditions. Considering real engine environments, they should also be integrated into computational fluid dynamics (CFD) frameworks.

4. Application of Syngas in Internal Combustion Engines

4.1. Application of Syngas in SI Internal Combustion Engines

Complete substitution of conventional fuels with syngas in SI engines is technically feasible, but direct operation of a naturally aspirated SI engine on syngas typically results in a 20–30% power loss due to its LHV compared to natural gas (~37 MJ/kg). To mitigate this limitation, blending syngas with high-LHV fuels (e.g., gasoline, natural gas, hydrogen) has been extensively investigated [104,105].

Fan et al. [106] investigated the enrichment of gasoline with syngas fractions up to 20% (with a hydrogen-to-carbon monoxide mass ratio of FH_2/FCO = 0.3/0.7). Their results showed that this enrichment increased both cylinder pressure and thermal efficiency. As expected, pure gasoline produced the highest nitrogen oxide (NOx) emissions. Increasing the proportion of syngas in the fuel blend generally reduced NOx emissions. Over the entire range of 0–20% syngas addition, the peak carbon monoxide (CO) mass increased steadily, while the carbon dioxide (CO_2) mass decreased.

Similarly, Chen et al. [93] reported that when the hydrogen-to-carbon monoxide mass ratio in syngas was FH_2/FCO = 0.5/0.5, increasing the syngas proportion in the blend reduced hydrocarbon (HC) emissions but gradually raised CO emissions.

CFD-based investigations have provided further insight into ignition timing and hydrogen fraction effects. Kan et al. [92] showed that syngas with higher H_2 content increases indicated thermal efficiency and reduces NOx compared to biogas, particularly under wide-open-throttle conditions. More recently, Park et al. [105] confirmed that syngas exhibits stable lean combustion with the lowest ignition failure limit among tested fuels (natural gas, ethanol, syngas), highlighting its suitability for ultra-lean operation.

Despite these benefits, complete reliance on syngas in SI engines may compromise power density, necessitating hybrid fuelling strategies [107–109]. Table 6 summarizes major recent studies on syngas utilization in SI engines, highlighting the trade-offs between efficiency, emissions, and engine modifications.

Table 6. Summary of research works on syngas utilization in SI engines.

Objective	Fuel Composition (% vol.)	Experimental Setup	Key Findings	Ref.
100% syngas in SI engine vs. gasoline	H_2: 13–19; CO: 16–24; CH_4: 1–6; CO_2: 9–14; N_2: balance	4−stroke, 1−cyl, 5.5 kW SI engine	↓ Power (~20%); ↑ CO_2; ↓ NOx & CO vs. gasoline	[110]
Syngas/CH_4/gasoline blends	H_2: 23–40; CO: 23–39; CH_4: 11–26; CO_2: 10–28	2−cyl Lombardini SI engine, 2000–4500 rpm	H_2−rich syngas improves efficiency; ↑ NOx; ↓ CO	[105]
Ignition timing & supercharging	H_2/CO ≈ 40/39; CH_4 traces	SI engine under boost & IT variation	↑ H_2, ↑ CO, ↓ CO_2 improve efficiency; supercharging ↑ NOx	[87]
CFD with hydrogen enrichment	H_2: 17; CO: 15; CH_4: 4; CO_2: 15; N_2: 53	4−cyl SI engine, 1500 rpm	↑ H_2 improves ITE; ↓ NOx vs. biogas	[92]
DI−SI syngas vs. CNG	H_2: 50; CO: 50 (+CH_4 20%)	1−cyl, DISI, CR = 14:1, 1500–2400 rpm	↑ Heat release & efficiency; ↓ torque vs. CNG	[104]
Equivalence ratio & CR effects	H_2: 60; CO: 40; LHV = 20.4 MJ/kg	1−cyl SI engine, CR = 9–11, 1200 rpm	↑ CR improves lean burn; syngas achieves lowest misfire limit	[111]
Producer gas in retrofitted CI → SI	H_2: 8.5; CO:30.5; CH_4: 0.3; CO_2: 4.8; N_2: 49.6	1−cyl CI engine, CR = 9–17, 1000–2000 rpm	↑ CR improves BTE (11→24%); ↓ smoke; ↑ CO	[17]
Stoichiometric vs. lean SG	H_2: 30; CO: 25; CO_2: 45	1−cyl CI engine, CR = 13–17, 1800 rpm	↑ CR increases ITE & HRR; ↓ combustion duration; ↓ gross power	[19]

Denotations: ↑: increase, ↓: decrease, ∼: nearly constant or insignificant,//: similar to above. BMEP: Brake Mean Effective Pressure, BTDC: Before Top Dead Center, BSFC: Brake Specific Fuel Consumption, IMEP: Indicated Mean Effective Pressure, CR: Compression Ratio, ITE: Indicated Thermal Efficiency, BTE: Brake Thermal Efficiency, CoV IMEP: Coefficient of Variation of IMEP, TC: Turbocharge, NA: Naturally Aspirated, IT: Ignition Timing, SOI: Start of Ignition, ϕ: the fuel/air equivalence ratio, WOT: Wide Open Throttle, and MBT: Maximum Brake Torque.

Overall, the studies summarized in Table 6 show that the main limitation of syngas in SI engines is its low energy density, which directly translates into reduced power output when used as the sole fuel. Hydrogen-rich syngas compositions help counter this drawback by improving lean-burn stability, ignition reliability, and thermal efficiency, but they cannot fully offset the loss in brake power. In practice, blending syngas with high-LHV fuels such as gasoline, natural gas, or hydrogen emerges as the most effective strategy to balance efficiency gains with manageable emissions. Importantly, compression ratio adjustments, ignition timing, and supercharging can further tailor performance, but their effects are highly engine-specific. Looking ahead, hybrid fueling strategies and advanced combustion control, supported by predictive CFD and AI models, offer promising pathways to unlock syngas potential in SI applications while minimizing its intrinsic power penalties.

4.2. Application of Syngas in CI Engines

CI engines are well-suited for syngas utilization due to their high efficiency and robustness. However, because of the high autoignition temperature of syngas, operation is typically carried out in DF mode, with diesel serving as the ignition pilot (10–20 vol.% of the fuel supply) [87,112]. Numerous studies confirm that DF syngas/diesel operation reduces soot emissions while maintaining power density. For instance, Aslam et al. [19] showed that syngas with higher H_2 fractions improves combustion efficiency and reduces CO and HC, though at the expense of increased NOx. Conversely, CO−rich syngas (>34%) lowers efficiency and increases emissions. Krishnamoorthi et al. [113] also found that H_2 enrichment boosts thermal efficiency but worsens NOx formation, whereas higher CO reduces NOx but increases incomplete combustion.

At low loads, syngas substitution can delay ignition and reduce efficiency due to its low reactivity [17]. Talibi et al. [114] demonstrated that CO_2 dilution within syngas significantly decreases combustion temperature, leading to lower NOx but higher CO and HC emissions. Recent simulation and experimental works confirm that optimized pilot injection strategies are crucial to balance efficiency and emission trade-offs.

Table 7 summarizes recent works on CI engines operating in DF mode with syngas, emphasizing the role of H_2/CO ratio, pilot fuel strategy, and load dependence.

Table 7. Summary of research works on syngas/diesel dual-fuel CI engines.

Objective	Fuel Composition (% vol.)	Experimental Setup	Key Findings	Ref.
Efficiency & emissions vs. H_2/CO ratio	H_2: 100–0; CO:0–100	Yanmar L100V CI, CR = 21.2:1	↑ H_2 → ↑ efficiency & NOx; ↑ CO → ↓ performance & NOx	[19]
Effect of load & H_2/CO ratio	H_2/CO = 100/0—0/100	Kirloskar CI, 1500 rpm, CR = 17.5:1	Max diesel replacement ~70%; H_2−rich → ↑ efficiency, ↑ NOx	[113]
CFD & exergy analysis of DF mode	H_2/CO ≈ 50/50	DF CI simulations	Syngas/diesel ↓ soot & CO; ↑ NOx at high load	[114]
PG/diesel dual mode	PG—H_2: 15–19; CO: 18–22; N_2: 45–55	Kirloskar CI, CR = 17:1	PG ↓ NOx & soot, but ↓ BTE	[17]
PG/diesel vs. PG/biodiesel DF	PG—H_2: 12; CO: 10; CH_4: 1.5; CO_2: 15; N_2: 59	1−cyl Kirloskar AV1 CI, CR = 5–20, 1450–1600 rpm	DF feasible without mods; BTE order: BD > D > D/PG > BD/PG; BD/PG ↓ smoke by 16%	[22]
Pilot injection optimization	PG—H_2: 20; CO: 20; N_2: 60	AVL 5402 CI, 1500 rpm	Split injection ↑ efficiency; ↓ emissions	[115]
PG + biodiesel (DiSOME) DF	PG—H_2: 15–19; CO: 18–22; N_2: 45–55	Apex CI engine, CR = 17.5:1, 1500 rpm	DF ↑ BTE by ~6%; ↓ HC & CO; ↑ NOx vs. HCCI	[116]
Modified DF diesel with PG	PG—H_2: 15–19; CO: 18–22; N_2: 45–55	Kirloskar TAF−1 CI, CR = 17:1, 1500 rpm	PG ↓ BTE, ↑ fuel consumption, ↓ NOx & HC	[117]
H_2 vs. PG DF	H_2: 100 PG—H_2: 15–19; CO: 18–22; N_2: 45–55	DF CI	H_2 → ↑ BTE, ↓ fuel use, ↑ HRR; PG → ↓ BTE, ↑ CO & HC	[118]

Denotations: ↑: increase, ↓: decrease, ∼: approximately constant, IMEP: Indicated Mean Effective Pressure, CR: Compression Ratio, HC: Hydrocarbon, HSDI: High-Speed Direct Injection, ITE: Indicated Thermal Efficiency, BTE: Brake Thermal Efficiency, BTDC: Before Top Dead Center, φ: air-fuel equivalence ratio, COVIMEP: Coefficient of IMEP, and UHC: Unburned Hydrocarbon.

In contrast to SI engines, where power density is the dominant concern, CI engines face challenges primarily related to ignition control and emissions management. The findings in Table 6 consistently indicate that H_2−rich syngas improves combustion efficiency and brake thermal efficiency but at the cost of higher NOx, while CO−rich or N_2−diluted syngas mitigates NOx but compromises efficiency through incomplete combustion. A recurring theme is the decisive role of pilot injection strategies, which strongly influence the trade-off between efficiency and emissions. Load dependence also emerges as a critical factor: syngas performs well at medium-to-high loads, but ignition delays and efficiency penalties persist at low loads. These insights suggest that the practicality of CI engines lies not in maximizing syngas substitution, but in flexible DF operation tuned to both syngas composition and engine load. Future progress will likely depend on adaptive pilot injection and predictive control methods, potentially AI-enhanced, that can stabilize combustion and minimize emissions variability in real-world conditions.

4.3. Critical Insights on Engine Applications

The application of syngas in ICEs demonstrates both potential and limitations. Across SI studies, there is broad agreement that moderate hydrogen fractions (15–35 vol%) improve ignition stability and flame propagation, while CO_2 and N_2 dilution reduce NOx by lowering flame temperature [90]. However, contradictions persist regarding the net effect of hydrogen enrichment on emissions. Some CFD studies report increased NOx at higher H_2 contents due to higher peak temperatures, while others observe reduced NOx under lean conditions, where faster burning shortens residence time at elevated temperatures. These discrepancies emphasise the strong dependence on equivalence ratio, operating load, and dilution levels.

In CI and DF configurations, syngas is often praised for lowering NOx when displacing part of the diesel pilot, but several studies highlight efficiency penalties and higher CO or unburned hydrocarbons, especially at high substitution levels [88,89]. This indicates that dual-fuel operation offers environmental benefits but requires optimisation of injection timing and substitution ratios to mitigate drawbacks.

HCCI studies remain relatively scarce, and most rely on simplified single-zone or multi-zone models. These show that syngas addition delays ignition and reduces peak cylinder pressures, thereby lowering NOx, but at the expense of higher CO and HC emissions. A key gap here is the lack of full-cycle CFD modelling under HCCI conditions, which would provide a more realistic assessment of combustion phasing and control challenges [106].

A broader methodological issue across engine studies is the frequent use of synthetic syngas mixtures with hydrogen levels far above those typically obtained from biomass gasification (>50 vol%) [119]. Such compositions yield optimistic performance predictions but have limited practical relevance. This disconnect underscores the need for future work to employ realistic gasification-derived syngas compositions and to systematically compare results across SI, CI, DF, and HCCI engines [71].

5. Discussion

The reviewed literature highlights both the promise and the challenges of syngas as a renewable fuel for internal combustion engines. Several cross-cutting themes emerge, but contradictions, methodological issues, and knowledge gaps also persist. These are summarised below:

- Syngas composition variability as a central challenge: The variability of syngas composition, dictated by feedstock and gasification process conditions, is consistently identified as a major factor influencing ignition delay, flame speed, and emissions. Moderate hydrogen contents (15–35 vol%) generally improve combustion stability, while CO_2 and N_2 act as diluents, lowering flame temperature and NOx emissions [66,90]. However, syngas produced from air-blown gasifiers is often nitrogen-rich, leading to significantly lower LHVs compared to oxygen/steam gasification pathways [33]. This compositional diversity complicates direct comparison between studies and limits the generalisation of results.
- Contradictions in the effect of hydrogen enrichment: Hydrogen is widely acknowledged as the most influential component of syngas due to its high diffusivity and reactivity. Most studies report that increasing H_2 reduces ignition delay and enhances flame speed [90,120]. Yet the effect on NOx emissions remains inconsistent: some works show higher H_2 fractions increase NOx due to higher flame temperatures [66], while others find the opposite under lean conditions, where faster burning reduces residence times at peak temperatures [86]. These contradictory findings highlight the strong dependence on boundary conditions, especially equivalence ratio and dilution levels.

- The dual role of carbon monoxide: Carbon monoxide contributes to syngas calorific value and participates in chain-branching reactions. Certain studies indicate that CO stabilises combustion and supports flame propagation [66,121], while others report inhibitory effects at high concentrations, reducing reactivity and prolonging ignition delay [78,93]. These contradictions can be attributed to the balance between CO's role as a reactive species and its competition with H_2 for oxidants. More systematic work under engine-relevant conditions is needed to clarify its role.
- Limitations of current kinetic and CFD models: Despite significant progress, kinetic mechanisms often fail to consistently predict laminar flame speeds and ignition delays across the full range of syngas compositions. Han et al. [121] showed that H_2/CO mechanisms underpredict LFS in CO_2-diluted mixtures at high pressure, necessitating refined rate constants. CFD simulations; meanwhile, frequently employ synthetic syngas mixtures with unrealistically high hydrogen contents (>50 vol%), which do not represent biomass gasification products [91]. Furthermore, turbulence–chemistry interaction models are often oversimplified, potentially compromising accuracy in transient or stratified combustion modes.
- Underexplored engine concepts and integration gaps: Most syngas research focuses on SI engines, with fewer studies addressing CI and dual-fuel strategies. Recent CFD studies suggest that direct-injection syngas operation in CI engines can achieve high efficiency with lower NOx emissions [91], yet this area remains underexplored compared to SI applications. Dual-fuel approaches (diesel/syngas or diesel/producer gas) also show promise for efficiency gains and NOx reduction [88], but the trade-offs in brake thermal efficiency and CO/HC emissions are not well quantified. HCCI applications of syngas are even less studied, with most models limited to zero-dimensional thermochemical approaches. Finally, there is a lack of integration between gasification studies (which define syngas variability) and engine simulations, leaving a gap on these observations, future work should focus on validating kinetic mechanisms under engine-relevant pressures, temperatures, and diluted conditions. Realistic syngas compositions reflecting biomass gasification should be employed, avoiding hydrogen-rich synthetic mixtures. Greater attention is required for CFD studies on CI, DF, and HCCI engines, which remain underrepresented compared with SI research. Systematic comparisons and meta-analyses across studies are needed to reconcile contradictory findings, particularly regarding the effects of H_2 and CO on NOx. Finally, integrating gasification modelling with combustion simulations would provide end-to-end insights from feedstock to engine performance [66,119,122].

6. Conclusions

This review analyses and critically compares existing literature to show that understanding syngas from biomass gasification, including the gasification process, combustion kinetics, experimental characterisation, modelling, and engine applications, is essential for unlocking its potential as a renewable fuel for internal combustion engines.

Despite advances in CFD, data-driven, and machine learning approaches for optimising syngas production, variations in composition due to feedstock, gasifier design, and operating conditions remain, affecting heating value, hydrogen content, combustion stability, and emissions. While extensive experimental and modelling studies have advanced our understanding of oxidation kinetics, flame propagation, and dilution effects, current kinetic mechanisms often show inconsistency under engine-relevant pressures, temperatures, and realistic syngas mixtures.

Key findings indicate that H_2-rich syngas enhances ignition stability, lean-burn operability, and thermal efficiency, yet low energy density, emissions trade-offs, and reliance

on idealised mixtures limit practical adoption. Mitigation strategies include hydrogen-rich blends, elevated compression ratios, advanced direct injection, adaptive pilot injection, dual-fuel cycles, and onboard catalytic reforming. Research should prioritise realistic gasification-derived compositions, refined kinetic models, AI-driven engine management, and hybridised systems to fully exploit syngas's potential in sustainable power generation and transport.

Author Contributions: Conceptualization, J.R.C.R.; Validation, C.N.; Resources, P.B.; Writing—original draft preparation, J.R.C.R., B.R., P.B. and C.N.; Writing—review and editing, J.R.C.R., A.L., C.M.-P. and C.N.; All authors have read and agreed to the published version of the manuscript.

Funding: This work was funded by Fundação para a Ciência e Tecnologia, I.P. (Portuguese Foundation for Science and Technology) under project UIDB/05064/2020 (VALORIZA—Research Center for Endogenous Resource Valorization).

Data Availability Statement: All data presented in this study are included in the article. Further inquiries can be directed to the corresponding author.

Conflicts of Interest: The authors declare no conflicts of interest.

References

1. Igini, M. Martina Igini Fossil Fuels Accounted for 82% of Global Energy Mix in 2023 Amid Record Consumption: Report. *Earth.Org*. 16 June 2024. Available online: https://earth.org/Fossil-Fuel-Accounted-for$-$82$-$of$-$Global-Energy-Mix-in$-$2023$-$Amid-Record-Consumption-Report/ (accessed on 20 August 2025).
2. IRENA. *Renewable Capacity Statistics 2025*; International Renewable Energy Agency: Abu Dhabi, United Arab Emirates, 2025.
3. Toscano, G.; De Francesco, C.; Gasperini, T.; Fabrizi, S.; Duca, D.; Ilari, A. Quality Assessment and Classification of Feedstock for Bioenergy Applications Considering ISO 17225 Standard on Solid Biofuels. *Resources* **2023**, *12*, 69. [CrossRef]
4. Shen, Y. Biomass Pretreatment for Steam Gasification toward H2-Rich Syngas Production—An Overview. *Int. J. Hydrogen Energy* **2024**, *66*, 90–102. [CrossRef]
5. Barskov, S.; Zappi, M.; Buchireddy, P.; Dufreche, S.; Guillory, J.; Gang, D.; Hernandez, R.; Bajpai, R.; Baudier, J.; Cooper, R.; et al. Torrefaction of Biomass: A Review of Production Methods for Biocoal from Cultured and Waste Lignocellulosic Feedstocks. *Renew. Energy* **2019**, *142*, 624–642. [CrossRef]
6. Wang, C.; Zhu, W.; Fan, X. Char Derived from Sewage Sludge of Hydrothermal Carbonization and Supercritical Water Gasification: Comparison of the Properties of Two Chars. *Waste Manag.* **2021**, *123*, 88–96. [CrossRef]
7. Mu, Q.; Aleem, R.D.; Liu, C.; Elendu, C.C.; Cao, C.; Duan, P.G. Oxygen Blown Steam Gasification of Different Kinds of Lignocellulosic Biomass for the Production of Hydrogen-Rich Syngas. *Renew. Energy* **2024**, *232*, 121132. [CrossRef]
8. Ghodke, P.K.; Sharma, A.K.; Jayaseelan, A.; Gopinath, K.P. Hydrogen-Rich Syngas Production from the Lignocellulosic Biomass by Catalytic Gasification: A State of Art Review on Advance Technologies, Economic Challenges, and Future Prospectus. *Fuel* **2023**, *342*, 127800. [CrossRef]
9. Widjaya, E.R.; Chen, G.; Bowtell, L.; Hills, C. Gasification of Non-Woody Biomass: A Literature Review. *Renew. Sustain. Energy Rev.* **2018**, *89*, 184–193. [CrossRef]
10. Valizadeh, S.; Khani, Y.; Farooq, A.; Kumar, G.; Show, P.L.; Chen, W.H.; Lee, S.H.; Park, Y.K. Microalgae Gasification over Ni Loaded Perovskites for Enhanced Biohydrogen Generation. *Bioresour. Technol.* **2023**, *372*, 128638. [CrossRef]
11. Akca, O.; Chen, J.; Dai, L.; Cobb, K.; Cheng, Y.; Chen, P.; Lei, H.; Ruan, R. Improving Carbon-Reduced Catalytic Gasification of Microalgae for Biohydrogen Production. *Algal Res.* **2024**, *84*, 103797. [CrossRef]
12. Śpiewak, K. Gasification of Sewage Sludge—A Review. *Energies* **2024**, *17*, 4476. [CrossRef]
13. Brandstätter, G.; Fürsatz, K.; Long, A.; Hannl, T.K.; Schubert, T. Exploring the Potential of Sewage Sludge for Gasification and Resource Recovery: A Review. *Environ. Technol. Innov.* **2025**, *40*, 104346. [CrossRef]
14. Alves, C.T.; Onwudili, J.A.; Ghorbannezhad, P.; Kumagai, S. A Review of the Thermochemistries of Biomass Gasification and Utilisation of Gas Products. *Sustain. Energy Fuels* **2023**, *7*, 3505–3540. [CrossRef]
15. Chang, Y.-J.; Chang, J.-S.; Lee, D.-J. Gasification of Biomass for Syngas Production: Research Update and Stoichiometry Diagram Presentation. *Bioresour. Technol.* **2023**, *387*, 129535. [CrossRef]
16. Susastriawan, A.A.P.; Saptoadi, H. Purnomo Small-Scale Downdraft Gasifiers for Biomass Gasification: A Review. *Renew. Sustain. Energy Rev.* **2017**, *76*, 989–1003. [CrossRef]
17. Rosha, P.; Dhir, A.; Mohapatra, S.K. Influence of Gaseous Fuel Induction on the Various Engine Characteristics of a Dual Fuel Compression Ignition Engine: A Review. *Renew. Sustain. Energy Rev.* **2018**, *82*, 3333–3349. [CrossRef]

18. Rinaldini, C.A.; Allesina, G.; Pedrazzi, S.; Mattarelli, E.; Savioli, T.; Morselli, N.; Puglia, M.; Tartarini, P. Experimental Investigation on a Common Rail Diesel Engine Partially Fuelled by Syngas. *Energy Convers. Manag.* **2017**, *138*, 526–537. [CrossRef]
19. Aslam, Z.; Li, H.; Hammerton, J.; Andrews, G.E. Combustion and Emissions Performance of Simulated Syngas/Diesel Dual Fuels in a CI Engine. In Proceedings of the SAE Powertrains, Fuels & Lubricants Conference & Exhibition, Krakow, Poland, 6–8 September 2022; SAE International: Warrendale, PA, USA, 2022.
20. Arslan, A.; Dev, S.; Yousefi, A.; Stevenson, D.; Liko, B.; Butler, J.; Guo, H.; Birouk, M. Combustion and Emission Performance of a Syngas-Diesel Dual-Fuel Generator. In Proceedings of the ASME 2022 ICE Forward Conference, Indianapolis, IN, USA, 16–19 October 2022; Volume 86540, p. V001T01A006.
21. Kumar, A.; Mounaïm-rousselle, C.; Brequigny, P.; Dhar, A.; Hespel, C.; Patel, C.; Kumar, D.; Duraisamy, G.; Le, L.; Sharma, N.; et al. Future of Internal Combustion Engines Using Sustainable, Scalable, and Storable E-Fuels and Biofuels for Decarbonizing Transport and Enabling Advanced Combustion Technologies. *Prog. Energy Combust. Sci.* **2025**, *110*, 101236. [CrossRef]
22. Sharma, P.; Sharma, A.K.; Ağbulut, Ü. A Comprehensive Review on Biomass-Derived Producer Gas as an Alternative Fuel: A Waste Biomass-to-Energy Perspective. *J. Therm. Anal. Calorim.* **2025**, *150*, 8913–8932. [CrossRef]
23. Bongomin, O.; Nzila, C.; Mwasiagi, J.I.; Maube, O. Exploring Insights in Biomass and Waste Gasification via Ensemble Machine Learning Models and Interpretability Techniques. *Int. J. Energy Res.* **2024**, *2024*, 6087208. [CrossRef]
24. Kumar, S.; Palange, R.; De Blasio, C. Advancements in Gasification Technologies: Insights into Modeling Studies, Power-to-X Applications and Sustainability Assessments. *Sustain. Energy Fuels* **2025**, *9*, 4793–4831. [CrossRef]
25. Jayanarasimhan, A.; Pathak, R.M.; Shivapuji, A.M.; Rao, L. Tar Formation in Gasification Systems: A Holistic Review of Remediation Approaches and Removal Methods. *ACS Omega* **2024**, *9*, 2060–2079. [CrossRef] [PubMed]
26. Jia, J.; Yan, X. Thermodynamic and Techno-Economic Analysis of a Biomass Gasification Tri-Generation System with Internal Combustion Engine and Stirling Engine. *Int. J. Hydrogen Energy* **2025**, *134*, 128–138. [CrossRef]
27. Copa, J.R.; Tuna, C.E.; Silveira, J.L.; Boloy, R.A.M.; Brito, P.; Silva, V.; Cardoso, J.; Eusébio, D. Techno-Economic Assessment of the Use of Syngas Generated from Biomass to Feed an Internal Combustion Engine. *Energies* **2020**, *13*, 3097. [CrossRef]
28. Suparmin, P.; Nurhasanah, R.; Nelwan, L.O.; Salleh, H.; Ridwan, M.; Anugerah, M. Syngas for Internal Combustion Engines, Current State, and Future Prospects: A Systematic Review. *Int. J. Automot. Mech. Eng.* **2024**, *21*, 11857–11876. [CrossRef]
29. Hydrogen Council. *Hydrogen Decarbonization Pathways*; Hydrogen Council: Brussels, Belgium, 2021.
30. Maitlo, G.; Ali, I.; Mangi, K.H.; Ali, S.; Maitlo, H.A.; Unar, I.N.; Pirzada, A.M. Thermochemical Conversion of Biomass for Syngas Production: Current Status and Future Trends. *Sustainability* **2022**, *14*, 2596. [CrossRef]
31. Samad, N.A.F.A. Effects of Different Gasifying Agents on Synthesis Gas Composition from Fluidized Bed Gasification Using Raw and Torrefied Wood Sawdust. *Chem. Eng. Trans.* **2024**, *114*, 1111–1116. [CrossRef]
32. Trejo, F. Review of Biomass Gasification Technologies with a Particular Focus on a Downdraft Gasifier. *Processes* **2025**, *13*, 2717. [CrossRef]
33. Gao, Y.; Wang, M.; Raheem, A.; Wang, F.; Wei, J.; Xu, D.; Song, X.; Bao, W.; Huang, A.; Zhang, S.; et al. Syngas Production from Biomass Gasification: Influences of Feedstock Properties, Reactor Type, and Reaction Parameters. *ACS Omega* **2023**, *8*, 31620–31631. [CrossRef]
34. Segneri, V.; Ferrasse, J.H.; Trinca, A.; Vilardi, G. An Overview of Waste Gasification and Syngas Upgrading Processes. *Energies* **2022**, *15*, 6391. [CrossRef]
35. Han, F.; Niu, Y.; Zhang, X.; Guo, Z.; Duan, S.; Liu, H.; Lu, B.; Chen, H. Performance Analysis of a Pilot Gasification System of Biomass with Stepwise Intake of Air-Steam Considering Waste Heat Utilization. *Renew. Energy* **2024**, *236*, 121498. [CrossRef]
36. Tezer, Ö.; Karabağ, N.; Öngen, A.; Çolpan, C.Ö.; Ayol, A. Biomass Gasification for Sustainable Energy Production: A Review. *Int. J. Hydrogen Energy* **2022**, *47*, 15419–15433. [CrossRef]
37. All Power Labs. The Five Processes of Gasification. Available online: https://www.allpowerlabs.com/gasification-explained (accessed on 20 August 2025).
38. Havilah, P.R.; Sharma, A.K.; Govindasamy, G.; Matsakas, L.; Patel, A. Biomass Gasification in Downdraft Gasifiers: A Technical Review on Production, Up-Gradation and Application of Synthesis Gas. *Energies* **2022**, *15*, 3938. [CrossRef]
39. Carmo-Calado, L.; Hermoso-Orzáez, M.J.; La Cal-Herrera, J.; Brito, P.; Terrados-Cepeda, J. Techno-Economic Evaluation of Downdraft Fixed Bed Gasification of Almond Shell and Husk as a Process Step in Energy Production for Decentralized Solutions Applied in Biorefinery Systems. *Agronomy* **2023**, *13*, 2278. [CrossRef]
40. Liu, G.; Zhang, R.; Sun, Z.; Zhang, B.; Wang, Z.; Liu, J.; Yang, B.; Wu, Z. Carbon-Negative Syngas Production: A Comprehensive Assessment of Biomass Pyrolysis Coupling Chemical Looping Reforming. *AIChE J.* **2023**, *69*, e18254. [CrossRef]
41. Miccio, F.; Polchri, L.; Murri, A.N.; Landi, E.; Medri, V. Chemical Looping Gasification of Biomass Char in Fluidized Bed and CO2-Enriched Atmosphere. *Biomass Convers. Biorefinery* **2025**, *15*, 11561–11571. [CrossRef]
42. Fang, S.; Zheng, X.; Lin, Y.; Ding, L.; Yan, S.; Li, J.; Huang, Z.; Huang, H. Evaluation of the Chemical Looping Gasification Characteristics of Kitchen Waste Using CuFe2O4 and NiFe2O4 as Oxygen Carriers. *Energy* **2024**, *312*, 133617. [CrossRef]

43. Mishra, S.; Upadhyay, R.K. Review on Biomass Gasification: Gasifiers, Gasifying Mediums, and Operational Parameters. *Mater. Sci. Energy Technol.* **2021**, *4*, 329–340. [CrossRef]
44. Kurkela, E. Pilot-Scale Development of Pressurized Fixed-Bed Gasification for Synthesis Gas Production from Biomass Residues. *Biomass Convers. Biorefinery* **2023**, *13*, 6553–6574. [CrossRef]
45. Meng, F.; Meng, J.; Zhang, D. Influence of Higher Equivalence Ratio on the Biomass Oxygen Gasification in a Pilot Scale Fixed Bed Gasifier. *J. Renew. Sustain. Energy* **2018**, *10*, 53101. [CrossRef]
46. Yao, X.; Zhao, Z.; Li, J.; Zhang, B.; Zhou, H.; Xu, K. Experimental Investigation of Physicochemical and Slagging Characteristics of Inorganic Constituents in Ash Residues from Gasification of Different Herbaceous Biomass. *Energy* **2020**, *198*, 117367. [CrossRef]
47. Hongrapipat, J.; Rauch, R.; Pang, S.; Liplap, P.; Arjharn, W.; Messner, M.; Henrich, C.; Koch, M.; Hofbauer, H. Co-Gasification of Refuse Derived Fuel and Wood Chips in the Nong Bua Dual Fluidised Bed Gasification Power Plant in Thailand. *Energies* **2022**, *15*, 7363. [CrossRef]
48. Jayah, T.H.; Aye, L.; Fuller, R.J.; Stewart, D.F. Computer Simulation of a Downdraft Wood Gasifier for Tea Drying. *Biomass Bioenergy* **2003**, *25*, 459–469. [CrossRef]
49. de Sales, C.A.V.B.; Maya, D.M.Y.; Lora, E.E.S.; Jaén, R.L.; Reyes, A.M.M.; González, A.M.; Andrade, R.V.; Martínez, J.D. Experimental Study on Biomass (Eucalyptus Spp.) Gasification in a Two-Stage Downdraft Reactor by Using Mixtures of Air, Saturated Steam and Oxygen as Gasifying Agents. *Energy Convers. Manag.* **2017**, *145*, 314–323. [CrossRef]
50. Couto, N.; Silva, V.; Cardoso, J.; Rouboa, A. 2nd Law Analysis of Portuguese Municipal Solid Waste Gasification Using CO2/Air Mixtures. *J. CO2 Util.* **2017**, *20*, 347–356. [CrossRef]
51. Luz, F.C.; Rocha, M.H.; Lora, E.E.S.; Venturini, O.J.; Andrade, R.V.; Leme, M.M.V.; Del Olmo, O.A. Techno-Economic Analysis of Municipal Solid Waste Gasification for Electricity Generation in Brazil. *Energy Convers. Manag.* **2015**, *103*, 321–337. [CrossRef]
52. Bhoi, P.R.; Huhnke, R.L.; Kumar, A.; Indrawan, N.; Thapa, S. Co-Gasification of Municipal Solid Waste and Biomass in a Commercial Scale Downdraft Gasifier. *Energy* **2018**, *163*, 513–518. [CrossRef]
53. Olgun, H.; Ozdogan, S.; Yinesor, G. Results with a Bench Scale Downdraft Biomass Gasifier for Agricultural and Forestry Residues. *Biomass Bioenergy* **2011**, *35*, 572–580. [CrossRef]
54. Onokwai, A.O.; Ajisegiri, E.S.A.; Okokpujie, I.P.; Ibikunle, R.A.; Oki, M.; Dirisu, J.O. Characterization of Lignocellulose Biomass Based on Proximate, Ultimate, Structural Composition, and Thermal Analysis. *Mater. Today Proc.* **2022**, *65*, 2156–2162. [CrossRef]
55. Lee, J.; Sohn, D.; Lee, K.; Park, K.Y. Solid Fuel Production through Hydrothermal Carbonization of Sewage Sludge and Microalgae Chlorella Sp. from Wastewater Treatment Plant. *Chemosphere* **2019**, *230*, 157–163. [CrossRef]
56. Alfarra, F.; Ozcan, H.K.; Cihan, P.; Ongen, A.; Guvenc, S.Y.; Ciner, M.N. *Artificial Intelligence Methods for Modeling Gasification of Waste Biomass: A Review*; Springer: Berlin/Heidelberg, Germany, 2024; Volume 196, ISBN 0123456789.
57. Alptekin, F.M.; Celiktas, M.S. Review on Catalytic Biomass Gasification for Hydrogen Production as a Sustainable Energy Form and Social, Technological, Economic, Environmental, and Political Analysis of Catalysts. *ACS Omega* **2022**, *7*, 24918–24941. [CrossRef]
58. Sakheta, A.; Raj, T.; Nayak, R.; O'Hara, I.; Ramirez, J. Improved Prediction of Biomass Gasification Models through Machine Learning. *Comput. Chem. Eng.* **2024**, *191*, 108834. [CrossRef]
59. Li, J.; Li, L.; Tong, Y.; Wang, X. Understanding and Optimizing the Gasification of Biomass Waste with Machine Learning. *Green Chem. Eng.* **2022**, *4*, 123–133. [CrossRef]
60. Yu, Z.; Wang, Z.; Zhong, H.; Cheng, K. Essential Aspects of the CFD Software Modelling of Biomass Gasification Processes in Downdraft Reactors. *RSC Adv.* **2024**, *14*, 28724–28739. [CrossRef] [PubMed]
61. Efremov, C.; Le, T.T.; Paramasivam, P.; Rudzki, K.; Osman, S.; Chau, T.H. Improving Syngas Yield and Quality from Biomass/Coal Co-Gasification Using Cooperative Game Theory and Local Interpretable Model-Agnostic Explanations. *Int. J. Hydrogen Energy* **2024**, *96*, 892–907. [CrossRef]
62. Li, J.; Suvarna, M.; Pan, L.-J.; Zhao, Y.; Wang, X. A Hybrid Data-Driven and Mechanistic Modelling Approach for Hydrothermal Gasification. *Appl. Energy* **2021**, *304*, 117674. [CrossRef]
63. Awais, M.; Omar, M.M.; Munir, A.; Li, W.; Ajmal, M.; Hussain, S.; Ahmad, S.A.; Ali, A. Co-Gasification of Different Biomass Feedstock in a Pilot-Scale (24 KWe) Downdraft Gasifier: An Experimental Approach. *Energy* **2022**, *238*, 121821. [CrossRef]
64. Xu, H.; Liu, F.; Sun, S.; Meng, S.; Zhao, Y. A Systematic Numerical Study of the Laminar Burning Velocity of Iso-Octane/Syngas/Air Mixtures. *Chem. Eng. Sci.* **2019**, *195*, 598–608. [CrossRef]
65. Nagar, V.; Kaushal, R. A Review of Recent Advancement in Plasma Gasification: A Promising Solution for Waste Management and Energy Production. *Int. J. Hydrogen Energy* **2024**, *77*, 405–419. [CrossRef]
66. Costa, M.; Piazzullo, D. The Effects of Syngas Composition on Engine Thermal Balance in a Biomass Powered CHP Unit: A 3D CFD Study. *Energies* **2024**, *17*, 738. [CrossRef]
67. Yin, G.; Wang, C.; Zhou, M.; Zhou, Y.; Hu, E.; Huang, Z. Experimental and Kinetic Study on Laminar Flame Speeds of Ammonia/Syngas/Air at a High Temperature and Elevated Pressure. *Front. Energy* **2022**, *16*, 263–276. [CrossRef]

68. Jithin, E.V.; Raghuram, G.K.S.; Keshavamurthy, T.V.; Velamati, R.K.; Prathap, C.; Varghese, R.J. A Review on Fundamental Combustion Characteristics of Syngas Mixtures and Feasibility in Combustion Devices. *Renew. Sustain. Energy Rev.* **2021**, *146*, 111178. [CrossRef]
69. Shang, R.; Zhuang, Z.; Yang, Y.; Li, G. Laminar Flame Speed of H2/CH4/Air Mixtures with CO2 and N2 Dilution. *Int. J. Hydrogen Energy* **2022**, *47*, 32315–32329. [CrossRef]
70. Wang, S.; Wang, Z.; Elbaz, A.M.; He, Y.; Chen, C.; Zhu, Y.; Roberts, W.L. Effects of CO2 Dilution and CH4 Addition on Laminar Burning Velocities of Syngas at Elevated Pressures: An Experimental and Modeling Study. *Energy Fuels* **2021**, *35*, 18733–18745. [CrossRef]
71. Kousheshi, N.; Yari, M.; Paykani, A.; Saberi Mehr, A.; de la Fuente, G.F. Effect of Syngas Composition on the Combustion and Emissions Characteristics of a Syngas/Diesel RCCI Engine. *Energies* **2020**, *13*, 212. [CrossRef]
72. Qian, Y.; Sun, S.; Ju, D.; Shan, X.; Lu, X. Review of the State-of-the-Art of Biogas Combustion Mechanisms and Applications in Internal Combustion Engines. *Renew. Sustain. Energy Rev.* **2017**, *69*, 50–58. [CrossRef]
73. Bhaduri, S.; Jeanmart, H.; Contino, F. EGR Control on Operation of a Tar Tolerant HCCI Engine with Simulated Syngas from Biomass. *Appl. Energy* **2018**, *227*, 159–167. [CrossRef]
74. Jothiprakash, G.; Balasubramaniam, P.; Sundaram, S.; Ramesh, D. Catalytic Biomass Gasification for Syngas Production: Recent Progress in Tar Reduction and Future Perspectives. *Biomass* **2025**, *5*, 37. [CrossRef]
75. Guo, P.; Liu, S.; Chang, X.; Wang, Z.; Xu, C.; Hu, L.; Lu, J. ScienceDirect The Synergistic Effect of Equivalence Ratio and Initial Temperature on Laminar Flame Speed of Syngas. *Int. J. Hydrogen Energy* **2022**, *47*, 23106–23117. [CrossRef]
76. Zhang, J.; Zhou, S.; Su, Y.; Luo, Z.; Wang, T. Experimental Study of the Influence of H_2/CO on the CH_4 Explosion Pressure and Thermal Behaviors. *ACS Omega* **2022**, *47*, 23106–23117. [CrossRef]
77. Nguyen, M.T.; Bui, V.G.; Nguyen, X.B.; Nguyen, L.C.T.; Pham, M.M.; Truong, T.H.; Phung, M.T.; Bui, V.H. Experimental Study of Explosion Characteristics and General Correlations of Lean H2/CO/CH4/Air Mixtures in Quiescence. *Int. J. Energy Res.* **2023**, *2023*, 8080573. [CrossRef]
78. Hamdy, M.; Abdelhalim, A.; Haque, M.A.; Abdelhafez, A.; Nemitallah, M.A. Flow, Combustion and Species Fields of Premixed CH_4/H_2/CO Syngas Oxy-Flames on a Swirl Burner: Effects of Syngas Composition. *Int. J. Hydrogen Energy* **2024**, *68*, 1398–1411. [CrossRef]
79. Wang, S.; Elbaz, A.M.; Wang, G.; Wang, Z.; Roberts, W.L. Turbulent Flame Speed of NH3/CH4/H2/H2O/Air-Mixtures: Effects of Elevated Pressure and Lewis Number. *Combust. Flame* **2023**, *247*, 112488. [CrossRef]
80. Zhao, H.; Yuan, C.; Li, G.; Tian, F. The Propagation Characteristics of Turbulent Expanding Flames of Methane/Hydrogen Blending Gas. *Energies* **2024**, *17*, 5997. [CrossRef]
81. Uka, D.; Blagojević, B.; Alioui, O.; Boublia, A.; Elboughdiri, N.; Benguerba, Y.; Jurić, T.; Popović, B.M. An Innovative and Environmentally Friendly Approach for Resveratrol Solubilization and Bioaccessibility Enhancement by Using Natural Deep Eutectic Solvents. *J. Mol. Liq.* **2023**, *391*, 123411. [CrossRef]
82. Hu, X.; Bai, F.; Yu, C.; Yan, F. Experimental Study of the Laminar Flame Speeds of the CH4/H2/CO/CO2/N2 Mixture and Kinetic Simulation in Oxygen-Enriched Air Condition. *ACS Omega* **2020**, *5*, 33372–33379. [CrossRef] [PubMed]
83. Burke, M.P.; Dryer, F.L.; Ju, Y. Assessment of Kinetic Modeling for Lean H2/CH4/O2/Diluent Flames at High Pressures. *Proc. Combust. Inst.* **2011**, *33*, 905–912. [CrossRef]
84. Kéromnès, A.; Metcalfe, W.K.; Heufer, K.A.; Donohoe, N.; Das, A.K.; Sung, C.J.; Herzler, J.; Naumann, C.; Griebel, P.; Mathieu, O.; et al. An Experimental and Detailed Chemical Kinetic Modeling Study of Hydrogen and Syngas Mixture Oxidation at Elevated Pressures. *Combust. Flame* **2013**, *160*, 995–1011. [CrossRef]
85. Li, X.; You, X.; Wu, F.; Law, C.K. Uncertainty Analysis of the Kinetic Model Prediction for High-Pressure H2/CO Combustion. *Proc. Combust. Inst.* **2015**, *35*, 617–624. [CrossRef]
86. Olm, C.; Zsély, I.G.; Varga, T.; Curran, H.J.; Turányi, T. Comparison of the Performance of Several Recent Syngas Combustion Mechanisms. *Combust. Flame* **2015**, *162*, 1793–1812. [CrossRef]
87. Costa, M.; La Villetta, M.; Massarotti, N.; Piazzullo, D.; Rocco, V. Numerical Analysis of a Compression Ignition Engine Powered in the Dual-Fuel Mode with Syngas and Biodiesel. *Energy* **2017**, *137*, 969–979. [CrossRef]
88. Wiemann, S.; Hegner, R.; Atakan, B.; Schulz, C.; Kaiser, S.A. Combined Production of Power and Syngas in an Internal Combustion Engine—Experiments and Simulations in SI and HCCI Mode. *Fuel* **2018**, *215*, 40–45. [CrossRef]
89. Costa, M.; Prati, M.V.; De Simio, L.; Iannaccone, S.; Piazzullo, D. CFD Study of a CI Engine Powered in the Dual-Fuel Mode with Syngas and Waste Vegetable Oil. *J. Phys. Conf. Ser.* **2021**, *1868*, 012014. [CrossRef]
90. Pérez Gordillo, D.S.; Mantilla González, J.M. Computational Study of the Effects of Ignition Parameters Changes on a Spark Ignition Engine Fueled With Syngas. *J. Energy Resour. Technol.* **2022**, *144*, 112306. [CrossRef]
91. Perrone, D.; Castiglione, T.; Morrone, P.; Pantano, F.; Bova, S. Energetic, Economic and Environmental Performance Analysis of a Micro-Combined Cooling, Heating and Power (CCHP) System Based on Biomass Gasification. *Energies* **2023**, *16*, 6911. [CrossRef]

92. Kan, X.; Zhou, D.; Yang, W.; Zhai, X.; Wang, C.-H. An Investigation on Utilization of Biogas and Syngas Produced from Biomass Waste in Premixed Spark Ignition Engine. *Appl. Energy* **2018**, *212*, 210–222. [CrossRef]
93. Chen, Q.; Zheng, Z.; Zhu, Z. Effects of Syngas Addition on Combustion Characteristics of Gasoline Surrogate Fuel. *ACS Omega* **2023**, *8*, 3929–3944. [CrossRef]
94. Shivapuji, A.M.; Dasappa, S. Influence of Fuel Hydrogen Fraction on Syngas Fueled SI Engine: Fuel Thermo-Physical Property Analysis and in-Cylinder Experimental Investigations. *Int. J. Hydrogen Energy* **2015**, *40*, 10308–10328. [CrossRef]
95. Gamiño, B.; Aguillón, J. Numerical Simulation of Syngas Combustion with a Multi-Spark Ignition System in a Diesel Engine Adapted to Work at the Otto Cycle. *Fuel* **2010**, *89*, 581–591. [CrossRef]
96. Shivapuji, A.M.; Dasappa, S. Selection and Thermodynamic Analysis of a Turbocharger for a Producer Gas-Fuelled Multi-Cylinder Engine. *Proc. Inst. Mech. Eng. Part A J. Power Energy* **2014**, *228*, 340–356. [CrossRef]
97. Kim, S.; Kim, J. Feasibility Assessment of Hydrogen-Rich Syngas Spark-Ignition Engine for Heavy-Duty Long-Distance Vehicle Application. *Energy Convers. Manag.* **2022**, *252*, 115048. [CrossRef]
98. Hariharan, D.; Rahimi Boldaji, M.; Yan, Z.; Mamalis, S.; Lawler, B. Single-Fuel Reactivity Controlled Compression Ignition through Catalytic Partial Oxidation Reformation of Diesel Fuel. *Fuel* **2020**, *264*, 116815. [CrossRef]
99. Olanrewaju, F.O.; Li, H.; Aslam, Z.; Hammerton, J.; Lovett, J.C. Analysis of the Effect of Syngas Substitution of Diesel on the Heat Release Rate and Combustion Behaviour of Diesel-Syngas Dual Fuel Engine. *Fuel* **2022**, *312*, 122842. [CrossRef]
100. Starik, A.M.; Korobov, A.N.; Titova, N.S. Combustion Improvement in HCCI Engine Operating on Synthesis Gas via Addition of Ozone or Excited Oxygen Molecules to the Charge: Modeling Study. *Int. J. Hydrogen Energy* **2017**, *42*, 10475–10484. [CrossRef]
101. Neshat, E.; Saray, R.K.; Hosseini, V. Effect of Reformer Gas Blending on Homogeneous Charge Compression Ignition Combustion of Primary Reference Fuels Using Multi Zone Model and Semi Detailed Chemical-Kinetic Mechanism. *Appl. Energy* **2016**, *179*, 463–478. [CrossRef]
102. Li, W.; Zou, C.; Yao, H.; Lin, Q.; Fu, R.; Luo, J. An Optimized Kinetic Model for H2/CO Combustion in CO2 Diluent at Elevated Pressures. *Combust. Flame* **2022**, *241*, 112093. [CrossRef]
103. Xia, W.; Huang, C.; Yang, J.; Zou, C.; Song, Y. Experimental and Modeling Study of Ignition Delay Times of Natural Gas with CO 2 Dilution. *Fuel* **2024**, *358*, 130148. [CrossRef]
104. Jamsran, N.; Park, H.; Lee, J.; Oh, S.; Kim, C.; Lee, Y.; Kang, K. Influence of Syngas Composition on Combustion and Emissions in a Homogeneous Charge Compression Ignition Engine. *Fuel* **2021**, *306*, 121774. [CrossRef]
105. Park, H.; Lee, J.; Jamsran, N.; Oh, S.; Kim, C.; Lee, Y.; Kang, K. Comparative Assessment of Stoichiometric and Lean Combustion Modes in Boosted Spark-Ignition Engine Fueled with Syngas. *Energy Convers. Manag.* **2021**, *239*, 114224. [CrossRef]
106. Fan, G.; Zheng, Z.; Zhu, Z. Combustion and Emission Characteristics of Gasoline Engine Blended Combustion Syngas. *ACS Omega* **2022**, *7*, 26375–26395. [CrossRef]
107. Caligiuri, C.; Baškovič, U.Ž.; Renzi, M.; Seljak, T.; Opresnik, S.R.; Baratieri, M.; Katrašnik, T. Complementing Syngas with Natural Gas in Spark Ignition Engines for Power Production: Effects on Emissions and Combustion. *Energies* **2021**, *14*, 3688. [CrossRef]
108. Bui, V.; Bui, T.M.T.; Tran, V.; Huang, Z.; Hoang, A.T.; Tarelko, W.; Bui, V.; Pham, X.M.; Nguyen, P.Q.P. Flexible Syngas-Biogas-Hydrogen Fueling Spark-Ignition Engine Behaviors with Optimized Fuel Compositions and Control Parameters. *Int. J. Hydrogen Energy* **2022**, *48*, 6722–6737. [CrossRef]
109. Bates, R.; Dölle, K. Syngas Use in Internal Combustion Engines—A Review. *Adv. Res.* **2017**, *10*, 1–8. [CrossRef]
110. Li, B.; Zhong, F.; Wang, R.; Jiang, Y.; Han, R. A Comparative Analysis of the Performances of a Syngas Port Injection plus Gasoline Direct Injection Combined-Injection Spark-Ignition Engine under Lean-Homogeneous Charge and Lean-Stratified Charge Modes. *Energy* **2024**, *308*, 132883. [CrossRef]
111. Zhang, Y.; Zhang, W.; Yu, B.; Li, X.; Zhang, L.; Zhao, Y.; Sun, S. Experimental and Kinetic Modeling Study on Laminar Flame Speeds and Emission Characteristics of Oxy-Ammonia Premixed Flames. *Int. J. Hydrogen Energy* **2024**, *63*, 857–870. [CrossRef]
112. de Campos, V.; Carmo-Calado, L.; Mota-Panizio, R.; Matos, V.; Silva, V.B.; Brito, P.S.; Eusébio, D.F.L.; Tuna, C.E.; Silveira, J.L. A Waste-to-Energy Technical Approach: Syngas–Biodiesel Blend for Power Generation. *Energies* **2023**, *16*, 7384. [CrossRef]
113. Krishnamoorthi, M.; Sreedhara, S.; Duvvuri, P.P. Experimental, Numerical and Exergy Analyses of a Dual Fuel Combustion Engine Fuelled with Syngas and Biodiesel/Diesel Blends. *Appl. Energy* **2020**, *263*, 114643. [CrossRef]
114. Talibi, M.; Hellier, P.; Ladommatos, N. Combustion and Exhaust Emission Characteristics, and in-Cylinder Gas Composition, of Hydrogen Enriched Biogas Mixtures in a Diesel Engine. *Energy* **2017**, *124*, 397–412. [CrossRef]
115. Lei, Y.; Wu, Y.; Qiu, T.; Zhou, D.; Lian, X.; Jin, W. Experimental Study of Dual-Fuel Diesel/Natural Gas High-Pressure Injection. *ACS Omega* **2023**, *8*, 519–528. [CrossRef]
116. Yaliwal, V.S.; Banapurmath, N.R.; Gaddigoudar, P.; Patil, N.D.; Harari, P.A. Performance and Emission Characteristics of a Diesel Engine Operated on Diverse Modes Using Renewable and Sustainable Fuels Derived from Dairy Scum and Municipal Solid Waste. *Mater. Today Proc.* **2021**, *47*, 2592–2597. [CrossRef]

117. Nguyen, V.N.; Nayak, B.; Singh, T.J.; Nayak, S.K.; Cao, D.N.; Le, H.C.; Nguyen, X.P. Investigations on the Performance, Emission and Combustion Characteristics of a Dual-Fuel Diesel Engine Fueled with Induced Bamboo Leaf Gaseous Fuel and Injected Mixed Biodiesel-Diesel Blends. *Int. J. Hydrogen Energy* **2024**, *54*, 397–417. [CrossRef]
118. Hosseini, S.H.; Tsolakis, A.; Alagumalai, A.; Mahian, O.; Lam, S.S.; Pan, J.; Peng, W.; Tabatabaei, M.; Aghbashlo, M. Use of Hydrogen in Dual-Fuel Diesel Engines. *Prog. Energy Combust. Sci.* **2023**, *98*, 101100. [CrossRef]
119. Saxena, M.; Ranjane, V.; Maurya, R. Crank Angle Based Exergy Analysis of Syngas Fuelled Homogeneous Charge Compression Ignition Engine. *SAE Tech. Pap.* **2022**, *01*, 1037. [CrossRef]
120. Martinez-boggio, S.; Lacava, P.T.; Carvalho, F.S. De Combustion Diagnosis in a Spark-Ignition Engine Fueled with Syngas at Different CO/H_2 and Diluent Ratios. *Gases* **2024**, *4*, 97–116. [CrossRef]
121. Han, W.; Dai, P.; Gou, X.; Chen, Z. A Review of Laminar Flame Speeds of Hydrogen and Syngas Measured from Propagating Spherical Flames. *Appl. Energy Combust. Sci.* **2020**, *1–4*, 100008. [CrossRef]
122. Ali, K.; Kim, C.; Lee, Y.; Oh, S.; Kim, K. A Numerical Study to Investigate the Effect of Syngas Composition and Compression Ratio on the Combustion and Emission Characteristics of a Syngas-Fueled HCCI Engine. *J. Energy Resour. Technol.* **2020**, *142*, 092301. [CrossRef]